

# Advanced Aerodynamic and Fault-Tolerant Control for VSVP Wind Turbines and DFIG Using Predictive and Sliding Mode Techniques

A.Ravi Shankar<sup>1\*</sup>, T.R.Jyothsna<sup>2</sup>

<sup>1</sup>Research Scholar, Electrical Engineering Department, Andhra University, Visakhapatnam, Andhra Pradesh, India<sup>1</sup>

<sup>2</sup>Electrical Engineering Department, Andhra University, Visakhapatnam, Andhra Pradesh, India<sup>2</sup>

\*shankar.alluri@gmail.com

---

## Article History:

Received: 12-01-2025

Revised: 15-02-2025

Accepted: 01-03-2025

## Abstract:

The integration of renewable energy systems, particularly Variable Speed Variable Pitch (VSVP) wind turbines, into the power grid is crucial for maximizing power generation efficiency and maintaining stability under fluctuating environmental conditions. However, challenges such as wind speed variations and grid disturbances affect their performance. This study proposes an advanced hybrid control framework to optimize aerodynamic performance, power capture, and fault resilience in Doubly Fed Induction Generator (DFIG)-based wind turbines. The primary objective of this research is to enhance power extraction efficiency and ensure robust Fault Ride-Through (FRT) capability by integrating Model Predictive Control (MPC) and Sliding Mode Control (SMC). MPC dynamically adjusts the pitch angle and generator torque, optimizing the power coefficient ( $C_p$ ) and reducing pitch angle deviation, rotor speed fluctuations, and response time. For fault mitigation during voltage dips, Higher-Order Sliding Mode Control (HOSMC) and the Super-Twisting Algorithm (STA) are implemented to regulate DFIG electromagnetic force, reducing torque ripples, voltage sags, and Total Harmonic Distortion (THD). The proposed framework is implemented using MATLAB. The power coefficient ( $C_p$ ) is improved to 0.52 at  $\lambda = 6.5$ , surpassing PI (0.42) and Fuzzy Logic (0.48) controllers. THD is reduced to 1.8%, compared to 3.5% (PI) and 2.3% (Fuzzy Logic), ensuring superior power quality. Torque ripple is minimized to 2.1%, enhancing turbine mechanical stability. The proposed strategy successfully improves FRT capability, enhances energy capture efficiency, and ensures grid stability. This dual-layer control framework offers a promising solution for improving the efficiency, reliability, and resilience of wind turbines under variable wind and grid conditions.

**Keywords:** Predictive Control, Sliding Mode Control, Variable Speed Variable Pitch Wind Turbines, DFIG, Voltage Dips

---

## 1. Introduction

Wind turbines have become essential elements for modern renewable energy systems because they need to connect seamlessly with electrical networks [1]. The power generation capabilities of Wind turbines with Variable Speed Variable Pitch configurations reach their optimal level through automated adjustments of operational features which match different wind conditions [2]. The control systems of VSVP wind turbines enable them to maximize power efficiency through active

adjustments of their blade pitch together with rotor speed [3]. The ability to adapt operation makes it possible to achieve maximum power and reduce component strain within wind turbines [4]. The modern electrical power grid persists multiple operational hurdles from adding variable renewable power sources especially wind energy generation [5]. Variable wind energy output generates power fluctuations which affect the stability of power grids while reducing their quality standards [6]. Electricity reliability suffers from voltage fluctuations that stem from quick wind speed alterations at the electrical supply level [7]. Modern wind turbines implement complex control systems together with power electronic converters which provide them with capability to operate over variable speeds under grid-friendly conditions [8]. The power electronic converters provide an operating separation between generators and grids through which turbines reach peak performance while delivering stability support through low voltage immunity features and reactive power control capabilities [9].

Proper wind energy integration to the power grid needs thoughtful scheduling and operational control systems [10]. The development process creates grid codes for wind farms to use when joining the grid through these specifications the power plants must enable reliable and stable operation. Current wind turbines include advanced features for providing essential ancillary services to balance frequency and support voltage requirements when disturbances happen in electrical networks [11], [12]. Prior power systems need better forecasting technologies as well as energy storage and smart grid technology to address supply stability problems caused by unpredictable power availability. Continuous investigation of wind turbine efficiency enhancement and power grid stability remains essential because wind energy utilization keeps growing. Research requires the comprehensive understanding of wind turbine-performance alongside grid-power distribution alongside environmental elements for developing efficient reliable systems [13]. The mitigation of these challenges will allow wind energy to sustain its essential function in the development of a sustainable renewable energy power grid.

### **1.1 Problem Statement**

The power extraction capability of VSVP wind turbines depends on pitch angle adjustments and generator torque control but the turbines become unstable due to unpredictable wind variations and grid breakdowns. Voltage dips affect DFIG-based wind turbines in a negative way because they create torque oscillations together with electromagnetic disturbances which degrade power quality [14]. The Proportional-Integral (PI) controllers face limitations in dealing with nonlinear processes and disturbances so powerful control strategies must exist to improve both system power performance and fault protection capabilities.

### **1.2 Existing Solutions & Limitations**

Multiple standard control techniques operate to regulate VSVP wind turbines together with DFIG systems. The widespread implementation of Proportional-Integral control stems from its easy use but it shows weaknesses when dealing with nonlinearities and grid incidents. The predictability of dynamic wind conditions remains limited when using Fuzzy Logic Control (FLC) systems because this method adapts well to uncertainties [15]. The real-time operating capacity of Adaptive Control comes at the cost of high computational complexity that prevents its practical use for real-time applications [16]. The robustness of Sliding Mode Control against nonlinearities causes the unwanted

side effect of chattering that negatively impacts system performance. The current control strategy requirements demand a superior method which provides optimized aerodynamic results and delivers reliable Fault Ride-Through capabilities to DFIG-based wind turbine applications during voltage drop events.

### 1.3 Research Motivation

This research introduces a dual-control approach combining Model Predictive Control with Advanced SMC features of Super-Twisting Algorithm and Higher-Order SMC to enhance power output and preserve power grid stability of DFIG-based wind turbines during faults. The proposed method aims to optimize aerodynamic efficiency through real-time MPC-based pitch and torque control. The system reaches higher FRT capability through STA-SMC for achieving smooth control activities along with HOSMC for reducing torque oscillations. Implement a system to minimize electromagnetic disturbances and enhance electric power quality when the power grid fails. The framework achieves maximum power output while providing grid stability because it combines multiple control techniques.

### 1.4 Research Significance

The research effectively optimizes the operational performance of DFIG-based wind turbines by handling wind speed fluctuations and grid interruption events. The developed framework reaches maximum energy collection efficiency through its real-time optimization of generator torque and pitch angle settings. This system design allows turbines to maintain stability when facing voltage dips while meeting all requirements of grid codes and strengthening power system stability. The introduced method operates to reduce Total Harmonic Distortion and decrease torque fluctuations, thus improving turbine operational efficiency and equipment lifetime duration. Renewable energy systems achieve enhanced electrical disturbance resistance by implementing the proposed power quality and grid integration method. The critical issues in wind energy systems require active resolution, leading to advanced wind power generation systems that operate more efficiently and handle faults better.

### 1.5 Key Contribution

The proposed study introduces a hybrid MPC + STA-SMC + HOSMC control approach, which addresses VSVP wind turbines and DFIG-based energy conversion systems. The key contributions are:

- ◆ MPC-based aerodynamic optimization for real-time pitch and torque control.
- ◆ Super-Twisting SMC for chattering-free voltage stabilization.
- ◆ Higher-Order SMC for minimizing electromagnetic torque ripple and THD.
- ◆ Enhanced fault ride-through capability for stable DFIG operation during grid voltage dips.
- ◆ Validated performance improvement through detailed simulation studies and comparative analysis.

The paper follows this structure: Section 1 explains the research problem alongside its motivation together with significance and key contributions. Section 2 reviews existing control strategies and their limitations. The control framework alongside modeling of the system appears within Section 3.

Results alongside comparative studies together with discussions are presented in Section 5 of the document. The section ends with essential outcomes along with proposed future research paths.

## 2. Related Works

Chen et al.,[17] develops a variable-speed control system which boosts power generation from three-turbine Savonius wind clusters through automatic phase angle adjustment elimination. The optimization process through Taguchi method analyses three major factors which include inter-turbine distances ( $L1 - 2, L1 - 3$ ), configuration angles ( $\theta1 - 2, \theta1 - 3$ ) and rotational direction. The research establishes that the average power coefficient raises by 1.425 as the wind ratio approaches 1.13, 1.14, and 1.09 when operating independently. The implementation of the system faces two main drawbacks because it can be impacted by variable wind conditions and struggles to scale up effectively as cluster sizes grow.

Research conducted by Gupta et al.,[18] focuses on investigating H-rotor Darrieus Vertical Axis Wind Turbines(VAWT) through active blade pitching techniques specifically for low wind speed areas. A high-fidelity 2D Computational Fluid Dynamics model simulates a variable blade pitching technique through sliding mesh and remising procedures for representing rotor rotational effects. A power coefficient ( $Cp$ ) value of 0.44 has been achieved through variable angle of attack adjustments for the NACA0015 airfoils at a tip speed ratio (TSR) level of 1.5, which yields an 81% enhancement. Performance upgrades can be achieved by lengthening blades together with increasing their number. Active pitching mechanisms must overcome two main limitations which include complicated aerodynamic effects between components and possible mechanical constraints during implementation.

Shan et al.,[19] demonstrated a new version of the Firefly Algorithm known as Parallel Compact Firefly Algorithm (PCFA) that optimizes performance through lower memory requirements. The compact technique reduces memory requirements which allows the technique to work for small-scale turbines at the same time as the parallel technique provides optimized solutions and faster solution times. PCFA used 28 benchmark functions as part of its testing before applying it to variable pitch wind turbine proportional–integral–derivative parameter tuning. PCFA demonstrates better performance than traditional compact optimization algorithms because it uses less memory and achieves superior solution quality and faster problem-solving speed. The control system achieves efficient output power control in wind turbines. The system demonstrates two main weaknesses which include its susceptibility to parameter adjustments and its computational difficulties in unstable operational environments.

The paper by Aghaeinezhad et al.,[20] presents AFO-NFTSMC an adaptive fractional-order non-singular fast terminal sliding mode controller for wind turbine individual pitch control against uncertainties and external disturbances: it is developed on a two-mass model of the wind turbine exists while using two separate subsystems to describe the aerodynamic parts and mechanical components and establishing related movement equations. The research adopts the single-blade method for controller evaluation using step and turbulent wind tests. FAST software and TurbSim simulation program serve to validate the system. The proposed controller delivers high precision performance together with enhanced stability when compared to conventional adaptive and sliding

mode controllers and demonstrates superior rotor speed tracking capabilities. The controller faces two drawbacks because it may require substantial computing capacity and it becomes challenging to implement in real time when wind conditions are severely fluctuating.

The study by LeBlanc et al.,[21] examines how changes in blade pitch affect a Vertical Axis Wind Turbine's (VAWT) structural and aerodynamic loads. Strain gauges measure blade normal loading through stressed struts during experiments at TU Delft's open jet wind tunnel under different fixed pitch offsets from a neutral position. The experimental results reveal how turbines respond sharply to pitch angle changes because they produce distinct aerodynamic phenomena, including blade dynamic stall along with blade vortex interaction. The adjustment of pitch controls rotor thrust characteristics while creating increased per-revolution response in loads that act on the rotor and platform acceleration frequencies. This analysis has experimental constraints, together with measurement error limitations that impact the scalability of real-life data.

The research of Palanimuthu [22] introduces the idea that Large-scale wind turbines can be made more reliable after simultaneous pitch actuator failures by using fault-tolerant finite-time constant non-singular terminal synergetic control manifolds. The control method adds enhanced accuracy to precision tracking processes together with reliable power regulation for extreme wind situations. A disturbance observer using mismatched control elements enhances the control system's ability to resist time-dependent disturbances while enhancing tracking capabilities. Stability and finite-time convergence are proved through the application of the Lyapunov theory. The simulation results measuring performance on 4.8 MW and 20 MW PMSG-based wind turbines demonstrate high reliability before and after disturbance occurrence. The system control faces some restrictions due to unpredictable modeling variations, practical deployment difficulties, and extreme operational disturbances that remain challenging for optimization.

The research by Chen et al.,[23] presents a self-adapting active fault-tolerant MPPT control method to protect maximum power point tracking capability in wind power systems through generator-side fault conditions. A specific observer component provides real-time estimation of perturbing effects generated by model uncertainties and nonlinearities together with unknown disturbances that incorporate failed generators and disturbance torque. An adaptive feedback linearizing control system controls the variable-speed wind turbine (VSWT) employing a compensation method applied to calculated perturbations. This system functions better than standard approaches because it works without modeling total systems accurately or precise measurement of all states or fault recognition methods. The three controller group shows better adaptability alongside better stability performance and diminishes tracking error compared to PI with NSSF-MPPT controllers. The proposed method demonstrates two crucial restrictions that include system-related fluctuations limitations plus necessary confirmation testing for external operational usage.

Song et al.,[24] suggest an adaptive switched sliding mode controller with the goal of enhancing the performance of floating wind turbines in the face of actuator failures and environmental uncertainty. The system is simulated by a switched linear model with average dwell time features, while mistakes, disturbances, and faults are managed via full-order state observers and adaptive laws. Three techniques are used in the work to generate control parameters: average dwell time, linear matrix inequality, and Lyapunov stability theory. The proposed controller successfully operates on

the *NREL 5MW* wind turbine with a spar-buoy platform through FAST simulations, which leads to superior power quality together with decreased mechanical loads compared to standard gain-scheduling PI control. The main constraints involve possible high computational demands as well as real-world offshore facility testing requirements.

Fayazi et al.,[25] recommended an L1 adaptive-sliding mode control (L1 adaptive-SMC) system which enhances wind turbine fault tolerance by managing pump wear and hydraulic leakage along with excessive air content in oil. A controller manages rotor speed and power regulation precisely through L1 adaptive control attached with sliding mode control containing adjustable gain and integrated sliding surface. The researchers performed validation using FAST simulations on a 5MW wind turbine at high wind speed operation. The results demonstrate how L1 adaptive-SMC provides superior performance compared to adaptive-SMC and adaptive control by enhancing system reliability during disturbances and faults as well as turbulent wind conditions.

Rodríguez et al.,[26] developed a Fault Detection and Diagnosis method based on Takagi-Sugeno Unknown Input Observer (TS-UIO) to track wind turbine active pitch system states under unknown uncertainties. Residual comparison between a TS-UIO and the system model enables sensor fault identification and detection through the approach. The method connects unknown inputs to Linear Matrix Inequalities, which leads to zero estimation error convergence. The simulation tests using reference wind turbine models show effective disturbance and noise performance. The main limitations originate from possible computational burden and the necessity of field tests to validate system effectiveness across diverse environmental conditions.

The study conducted by Aoun et al.,[27] explores field-oriented control techniques for active and reactive power regulation in doubly fed induction generators to improve energy quality in variable speed wind turbines. A comparison of neural network controllers, fuzzy logic controllers, and proportional-integral controllers was made through MATLAB/Simulink simulation tests. Standard guidelines were used to tune the PI controller, though its reduction needed high computational work. Mathematical stability proof was absent from the FLC despite its improved performance abilities. The dynamic response and tracking accuracy were superior when using a Neural Network Controller when compared to its counterparts. Challenges comprise the complications with Neural Network Controller training and the real-time validation required for actual wind farm operations.

Wang et al.,[28] studied mechanical-electrical-grid modeling of doubly fed induction generators to analyze grid stabilization and electrical damping under various wind speed and control parameters. This incorporates machine dynamics, electrical behavior, and grid interrelations, validated by simulation. The main findings are this: (1) Wind speed and control strategy influence shaft oscillations, and rotor-side impedance varies with wind speed; (2) For constant wind speeds, control parameters influence drive train dynamics, rotor-side impedance is mainly affected by proportional gains in the control system, offering insights for improving DFIG stability in grid integration. The limitations of this modeling are assumptions of the model and its need for real-world verification under changing grid conditions.

**Table 1: Literature Review**

Reference	Method	Findings	Limitations
Chen et al.,[17]	Variable-speed control for three-turbine Savonius wind cluster using the Taguchi method.	Optimized configuration improves power coefficient by 1.425 times compared to an isolated turbine at specific tip speed ratios.	Sensitivity to wind fluctuations and scalability concerns for larger clusters.
Gupta et al.,[18]	Active blade pitching for H-rotor Darrieus VAWTs using Computational Fluid Dynamics modeling.	Power coefficient of 0.44 achieved, increasing efficiency by 81% at TSR = 1.5.	Complex aerodynamic interactions and structural challenges in implementation.
Shan et al.,[19]	Parallel Compact Firefly Algorithm for PID tuning in variable pitch wind turbines.	PCFA reduces memory consumption, improves solution quality, and accelerates convergence.	Sensitivity to parameter settings and computational complexity in dynamic environments.
Aghaeinezhad et al.,[20]	Adaptive Fractional-Order Non-Singular Fast Terminal Sliding Mode Controller for pitch control.	Improved rotor speed tracking accuracy and stability under disturbances.	Computational complexity and challenges in real-time implementation under extreme wind variations.
LeBlanc et al.,[21]	Experimental analysis of blade pitch variations on VAWTs using wind tunnel tests.	Pitch adjustments influence aerodynamic effects, rotor thrust, and loading frequencies.	Experimental uncertainties and limitations in real-world scalability.
Palanimuthu[22]	Fault-tolerant synergetic control for large-scale wind turbines with pitch actuator faults.	Enhances precision tracking and stable power regulation under extreme wind conditions.	Modeling uncertainties and real-world implementation challenges.

Chen et al.,[23]	Adaptive active fault-tolerant MPPT control system for wind power under generator faults.	Improved robustness, reduced tracking errors, and better dynamic performance compared to traditional controllers.	Sensitivity to extreme variations and need for real-world validation.
Song et al.,[24]	Adaptive switched sliding mode controller for floating wind turbines.	Improved power quality and reduced mechanical loads compared to gain-scheduling PI control.	Computational complexity and need for validation in real offshore environments.
Fayazi et al.,[25]	L1 adaptive-sliding mode control for fault tolerance in wind turbines.	Ensures greater reliability under faults, disturbances, and turbulent wind conditions.	Complexity in implementation and need for real-world validation.
Rodríguez et al.,[26]	Fault Detection and Diagnosis using a Takagi-Sugeno Unknown Input Observer.	Robust fault detection and isolation in active pitch systems of wind turbines.	Computational complexity and need for real-world testing.
Aoun et al.,[27]	Comparison of PI, Fuzzy Logic, and Neural Network Controllers for DFIG wind turbines.	NNC provides better tracking accuracy and dynamic response than PI and FLC.	High computational effort required for training and real-time validation.
Wang et al.,[28]	Mechanical–electrical-grid model for DFIG stability analysis.	Wind speed and control strategy influence shaft oscillations, while control gains affect rotor-side impedance.	Model assumptions and need for real-world validation in grid conditions.

The literature reviewed addresses in table 1 contains numerous advancements in wind turbine control such as variable-speed control, active blade pitching, adaptive fault-tolerant methods, and

optimization strategies. Aerodynamic efficiency enhancements were investigated using Computational Fluid Dynamics, optimization techniques such as the Parallel Compact Firefly Algorithm, and fault-tolerant methods like Adaptive Fractional-Order Sliding Mode Control and L1 adaptive-sliding mode control. Nevertheless, there are loopholes in merging predictive control with sliding mode approaches for DFIG and Vertical Speed Variable Pitch wind turbines. Previous works are missing exhaustive fault-tolerant schemes fusing model predictive control and sliding mode control to promote reliability, flexibility, and resilience in the face of changing wind patterns and grid uncertainties.

### 3. System Modeling

The proposed wind energy conversion system uses Variable-Speed Variable-Pitch wind turbines together with Doubly Fed Induction Generators that operate under advanced hybrid control framework shown in Figure 1.

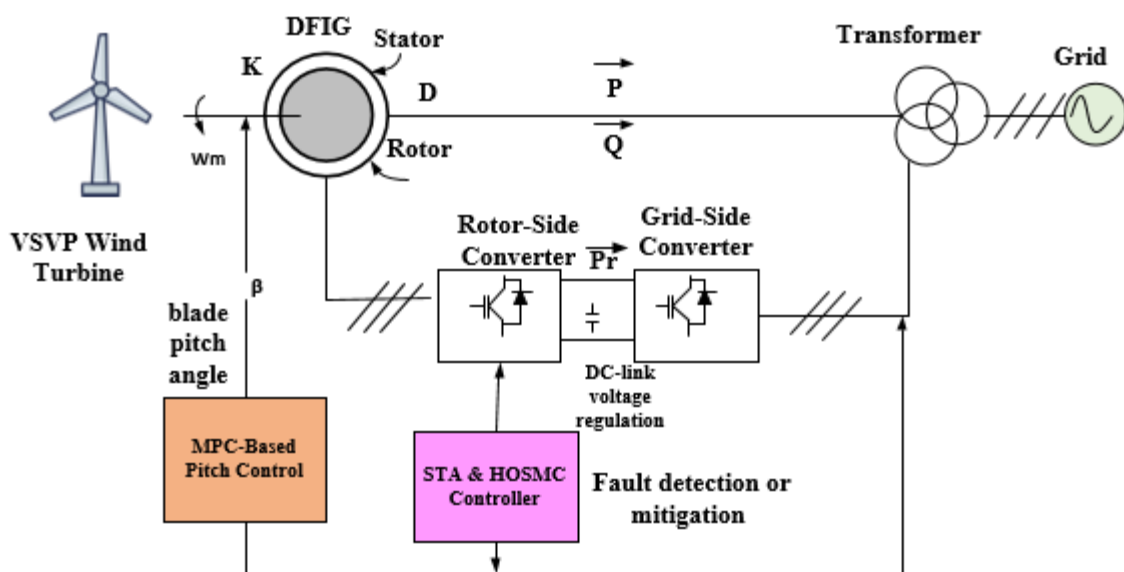


**Fig. 1. Proposed Framework**

The wind turbine model includes the basic steps of wind power extraction from aerodynamic resources. Two crucial elements of power coefficient efficiency control the ability of energy conversion. The DFIG model operates under two voltage equations which use the synchronous reference frame for rotational basis. Active and reactive power transfer relies on the converter systems found both on the rotor and on the grid side. The grid connects directly to the stator section yet the rotor section organizes power transfer through a back-to-back converter. This study integrates Model Predictive Control to optimize aerodynamics simultaneously with Sliding Mode Control through the combination of Super-Twisting Algorithm and Higher-Order SMC for fault tolerance. The MPC real-time system controls generator torque and pitch angle whereas STA-SMC operates as a voltage stabilizer which protects against grid disturbances. The unified modeling technique leads to optimized electrical power output alongside enhanced operational steadiness and improved connection with the power grid.

### 3.1 Variable Speed Variable Pitch Wind Turbine

The Variable Speed Variable Pitch Wind Turbine functions in a dynamic way with its rotational speed but also changes blade pitch angles to optimize power output under fluctuating wind conditions. The turbine operates with improved efficiency and reduced risk of mechanical damage due to stress injuries during powerful wind conditions because of its adaptive capabilities.

#### a) Aerodynamic Model of a Wind Turbine

The power generated by a wind turbine is given by the aerodynamic power equation:

$$O_d = \frac{1}{2} \rho A V_\omega^3 C_p(\lambda, \beta) \quad (1)$$

In Eqn. (1)  $O_d$  means power extracted from wind ( $W$ ),  $\rho$  is the air density ( $kg/m^3$ ),  $A$  means swept area of the rotor ( $\pi R^2$ ) ( $m^2$ ),  $V_\omega$  is the Wind speed ( $m/s$ ),  $C_p(\lambda, \beta)$  is the Power coefficient, dependent on tip-speed ratio ( $\lambda$ ) and pitch angle ( $\beta$ ). This equation shows that power extraction depends on wind speed, blade design, and control strategies (pitch and speed control).

#### b) Power Coefficient ( $C_p$ ) and Tip-Speed Ratio ( $\lambda$ )

The effectiveness of converting wind energy into mechanical energy is shown by the power coefficient  $C_p$  :

$$C_p(\lambda, \beta) = C_{p,max} \times f(\lambda, \beta) \quad (2)$$

In Eqn. (2)  $C_{p,max}$  is the maximum theoretical efficiency ( $\sim 0.59$ , *Betz limit*),  $f(\lambda, \beta)$  means empirical function relating  $C_p$  to  $\lambda$  and  $\beta$ . The following provides the tip-speed ratio ( $\lambda$ ) Eqn. (3).

$$\lambda = \frac{\omega_t B}{V_\omega} \quad (3)$$

Where,  $\omega_t$  is the rotor angular velocity,  $B$  means blade radius ( $m$ ),  $V_\omega$  refers to wind speed ( $m/s$ ).

#### c) Blade Pitch Angle ( $\beta$ ) Dynamics

Beta ( $\beta$ ) is dynamically adjusted by the pitch angle control to manage power output:

$$\frac{d\beta}{dt} = K_p (P_{ref} - P_t) + K_i \int (P_{ref} - P_t) dt \quad (4)$$

In Eqn. (4)  $P_{ref}$  represents reference power,  $K_p, K_i$  means proportional and integral gains for pitch control. Working if  $P_t > P_{ref}$  (excessive power),  $\beta$  increases, reducing  $C_p$  and limiting power. If  $P_t < P_{ref}$  decreases, increasing  $C_p$  and capturing more power.

#### d) Turbine Power Extraction Model

The mechanical torque produced by the turbine rotor is:

$$U_t = \frac{P_t}{\omega_r} = \frac{1}{2} \rho A v_\omega^3 \frac{C_p}{\omega_r} \quad (5)$$

In Eqn. (5)  $U_t$  means turbine torque ( $Nm$ ),  $\omega_r$  means rotor angular velocity ( $rad/s$ ). To achieve maximum operation: At low winds: Sustain maximum  $C_p$  by regulating tip-speed ratio  $\lambda$ . At high winds: Use pitch control ( $\beta$ ) to restrict power and avoid turbine overloading

### 3.2 Doubly Fed Induction Generator

During VSVP turbines, wind-speed variations induce a power-generation fluctuation, promoting mechanical stress, as well as lowering efficiency. A VSVP Wind Turbine is designed to operate dynamically at a rotational speed and to alter the blade pitch angle to maximize power generation over changing wind conditions. Such adaptability increases the efficiency of the turbine and protects it from injury due to excess mechanical stresses during high wind speeds. A Doubly Fed Induction Generator operates at variable speeds while maintaining grid coordinates. This makes it ideal for reliable and efficient wind energy conversion. It attained very high efficiency in power extraction as well as FRT capability, and it is further very ideal for reactive power control during voltage dips. For grid integration, it uses a partly rated power converter or cost-effective flexible inverter on grid features.

The wound rotor induction machine operates with the stator directly linked to the grid and a back-to-back converter manages power flow for the rotor to provide independent control. A Doubly Fed Induction Generator consists of a stator, directly connected to the grid, and a rotor, connected via a back-to-back converter. The Rotor-Side Converter (RSC) regulates rotor currents to control active and reactive power, while the Grid-Side Converter (GSC) maintains DC-link voltage and ensures power quality. In sub synchronous mode ( $\omega_r < \omega_s$ ), wind speed is less than the rated value, and the rotor takes power from the grid via RSC, while both the rotor and stator deliver power to the grid. In synchronous mode ( $\omega_r = \omega_s$ ), wind speed equals synchronous speed and only the stator supplies power. In super synchronous mode ( $\omega_r > \omega_s$ ), wind speed exceeds that rated value; the rotor injects power into the grid via RSC, with both the rotor and stator supplying power to the grid. DFIG's mathematical model has been developed in a synchronous  $dq$  reference frame where the d-axis is to stator flux.

#### a) Stator and Rotor Voltage Equations in $dq$ Reference Frame

DFIG is in synchronous  $dq$  reference frame, where voltages, currents, and flux linkages are expressed in direct-axis ( $d$ ) and quadrature-axis ( $q$ ) components is shown in Figure 2. In  $dq$  reference frame, the voltage equations of stator are as follows:

$$V_{ds} = R_s I_{ds} + \frac{d\psi_{ds}}{dt} - \omega_s \psi_{qs} \quad (6)$$

$$V_{qs} = R_s I_{qs} + \frac{d\psi_{qs}}{dt} - \omega_s \psi_{ds} \quad (7)$$

In Eqns. (6) and (7)  $V_{ds}, V_{qs}$  represents stator voltages ( $V$ ),  $I_{ds}, I_{qs}$  means stator currents (A),  $\psi_{qs}, \psi_{ds}$  is the stator flux linkages ( $Wb$ ),  $R_s$  means stator resistance ( $\Omega$ ),  $\omega_s$  is the synchronous angular velocity (rad/s). The rotor equations, again, expressed in the synchronous frame, are defined in Eqns. (8) and (9).

$$V_{dr} = R_r I_{dr} + \frac{d\psi_{dr}}{dt} - (\omega_s - \omega_r) \psi_{qr} \quad (8)$$

$$V_{qr} = R_r I_{qr} + \frac{d\psi_{qr}}{dt} - (\omega_s - \omega_r) \psi_{dr} \quad (9)$$

Where,  $V_{dr}, V_{qr}$  is the rotor  $dq$ -axis voltages( $V$ ),  $R_r$  means rotor resistance( $\Omega$ ).  $I_{dr}, I_{qr}$  is the rotor  $dq$ -axis currents( $A$ ),  $\Psi_{qr}, \Psi_{dr}$  represents rotor  $dq$ -axis flux linkages( $Wb$ ),  $\omega_s$  means synchronous speed( $rad/s$ ),  $\omega_r$  means rotor speed( $rad/s$ ),  $(\omega_s - \omega_r)$  means slip speed.

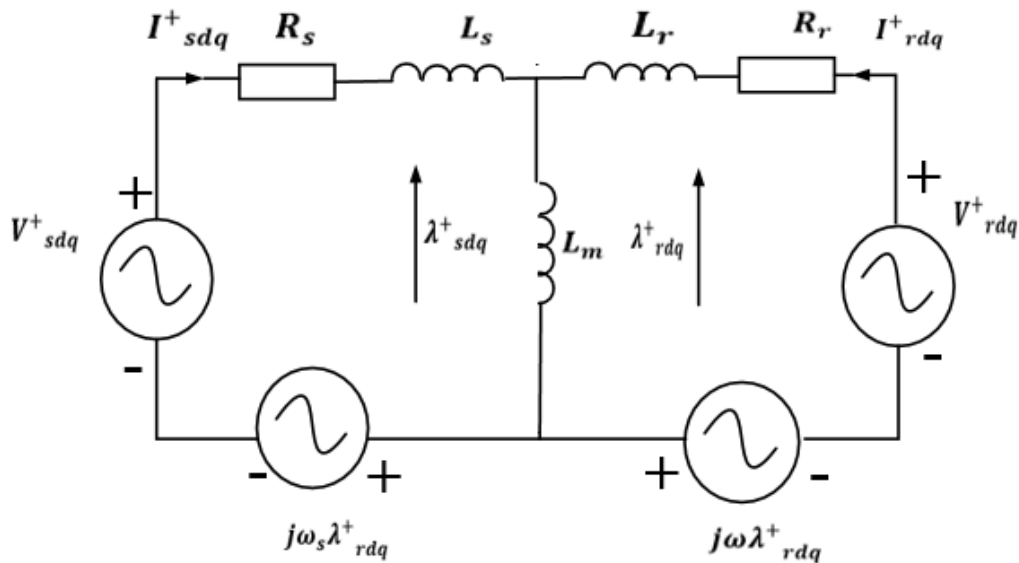


**Fig.2. dq Reference Frame**

Eqns. (10), (11), (12) and (13) are valid for stator and rotor flux linkages, respectively.

$$\Psi_{ds} = L_s I_{ds} + L_m I_{dr} \quad (10)$$

$$\Psi_{qs} = L_s I_{qs} + L_m I_{qr} \quad (11)$$

$$\Psi_{dr} = L_r I_{dr} + L_m I_{qs} \quad (12)$$

$$\Psi_{qr} = L_r I_{qr} + L_m I_{qs} \quad (13)$$

Here,  $L_s, L_r$  means Stator and rotor self-inductances ( $H$ ) and  $L_m$  refers to mutual inductance( $H$ ). The equation for the DFIG electromagnetic torque is given in Eqn. (14).

$$T_e = \frac{3P}{2} L_m (I_{qs} I_{dr} - I_{ds} I_{qr}) \quad (14)$$

Where  $T_e$  means electromagnetic torque ( $Nm$ ) and  $P$  is the number of poles. Generator Mode ( $T_e < 0$ ): Extracts energy from the wind where absorption of energy (not adopted in wind turbines). For example, in wind turbines, the generator mode converts mechanical power from wind into electrical power. Under grid voltage dips, DFIG response is the subject of many studies because of stator voltage drop, huge rotor currents, and torque oscillation. These problems might lead to rotor-side converter (RSC) arm breakdowns and, ultimately, turbine disconnection if left unattended. In this work, the implementation of Sliding Mode Control (SMC) integrated with the Super-Twisting Algorithm (STA) to alleviate this problem.

### 3.3 MPC-Based Aerodynamic Control for Power Optimization

The optimization process in VSVP wind turbines through Model Predictive Control achieves power extraction by maximizing power coefficient parameters with pitch angle and tip-speed ratio

regulations. According to the wind conditions, the controller shall adjust the pitch angle and generator torque adaptively to make the power conversion process at the highest efficiency. MPC aims to minimize ( $C_p$ ), by appropriately adjusting the pitch angle and generator torque ( $\tau_g$ ) in real-time. The formulation of MPC cost function is provided in Eqn. (15) MPC consists of solving an optimisation problem at time step  $k$  for a finite prediction horizon. The usual cost function of the MPC can be written as:

$$J = \sum_{k=0}^{N_p} (w_1(P_{ref} - P_w)^2 + w_2(\beta_k - \beta_{k-1})^2 + w_3(\tau_{g,k} - \tau_{g,k-1})^2) \quad (15)$$

Here,  $J$  is the cost function in this case to minimize,  $N_p$  Prediction horizon,  $w_1, w_2, w_3$  weighting factors. The terms  $P_{ref}$  and  $P_w$  denote reference power output, actual power extracted, and  $\beta_k, \beta_{k-1}$  as pitch angle at the current and prior time steps, respectively. Generator torque at the current and prior time steps, expressed as  $\tau_{g,k} - \tau_{g,k-1}$ . The first term minimizes the power tracking error so that the maximum power can be extracted. The second and third terms prevent mechanical stress on turbine components by ensuring that pitch and torque are varied smoothly. The Real-Time Optimization Problem the controller predicts future power output based on the state of the turbine and wind conditions. Similar to discretized state-space models used for turbine dynamics. The pitch system adjusts blades to maximize  $C_p$  in partial load conditions and limit power in full load conditions. The pitch angle ( $\beta^*$ ) and generator torque ( $\tau_g^*$ ) that minimize the cost function. To avoid excessive glide-pitch change and roll-axial torque change. In Control Action Execution, the first control input of the optimized sequence is applied. In partial load conditions, the pitch system adjusts the blades in such a way that it maximizes  $C_p$ , while maintaining  $P$  power below the maximum power in full load conditions. At the subsequent time step, it re-solves the optimization problem in light of newly received measurements. Maintaining Steady Pitch Control and Torque Adjustments a state-space model for pitch control is given as:

$$\beta = \frac{1}{T_p} (\beta - \beta^*) \quad (16)$$

In Eqn. (16)  $T_p$  is the pitch actuator time constant. Generator Torque Control is denoted in Eqn. (17). The generator torque reference is adjusted to match the optimal torque-speed curve:

$$\tau_g = k_{opt} \omega_r^2 \quad (17)$$

Where  $k_{opt}$  is an empirical constant based on turbine characteristics. The data on system predictions of its future behavior, control inputs, and optimal adjustments Pitch overshoot, mechanical wear, pitch response, and powering efficiencies Predictive analytics for wind response and grid integration

### 3.4 Sliding Mode Control Techniques for Fault-Tolerant DFIG Control

The main goal of Sliding Mode Control is Fault Ride-Through capability in the DFIG system, providing stability and effectiveness under grid voltage dip and disturbance conditions. Traditional control strategies do not work properly during grid faults and instead produce torque oscillations, high THD, and voltage instability. SMC is preferred because it responds quickly, is insensitive to uncertainties, and can deal with nonlinearities. The two most prominent SMC methods employed for fault-tolerant control of DFIG are: Super-Twisting Algorithm-Based SMC Minimizes chattering and

improves voltage stability. Higher-Order Sliding Mode Control Controls electromagnetic torque, reduces torque ripples, and provides robust current and voltage regulation.

### 3.4.1 Super-Twisting Algorithm

The chattering problem, which results in excessive control effort and mechanical wear, is a standard feature of SMC. An STA, a Second-Order Sliding Mode, can solve this problem by enabling a smooth control action while preserving resilience and reducing chattering.

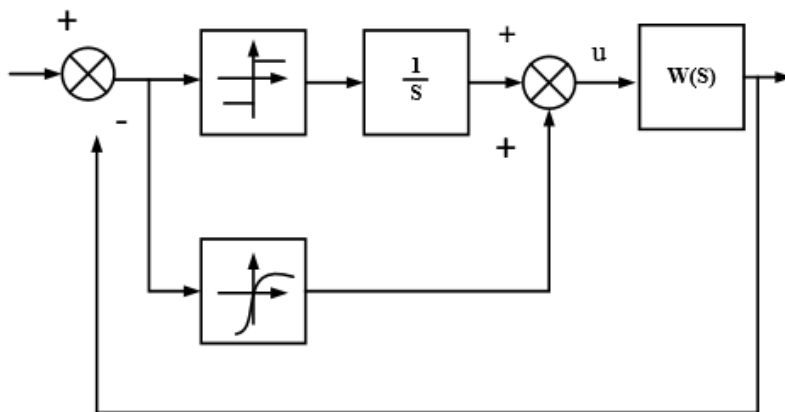


**Fig. 3. Super-Twisting Algorithm**

Consider the DFIG rotor current control under a voltage dip. The rotor current dynamics in the  $dq$  reference frame are given by Eqn. (18).

$$\frac{di_r}{dt} = -\frac{R_r}{L_r}i_r + \frac{1}{L_r}(v_r - j\omega_s\psi_r) \quad (18)$$

Where,  $i_r = i_{rd} + ji_{rq}$  rotor currents in the  $dq$  reference frame,  $R_r, L_r$  means rotor resistance and inductance,  $v_r = v_{rd} + jv_{rq}$  rotor voltage,  $\omega_s$  refers to synchronous speed,  $\psi_r$  means rotor flux. To regulate the rotor current, define the sliding surface as:

$$S = i_r - i_r^* \quad (19)$$

In Eqn. (19)  $i_r^*$  is the reference rotor current. The control objective is to drive  $S$  to zero, ensuring accurate current tracking. The STA-SMC control input is designed as Eqn. (20)

$$v_r = -k_1|S|^{1/2}sign(S) - k_2\int sign(S)dt \quad (20)$$

Where,  $k_1, k_2$  means positive control gain that can guarantee fast convergence, and  $sign(S)$  is the sign function that acts to implement the sliding mode. The benefits of STA-SMC for DFIG are that it reduces chattering, ensuring smooth control action. Enhances voltage stability by stabilizing the rotor current under grid faults. Faster response compared to conventional SMC.

### 3.4.2 Higher-Order Sliding Mode Control

With the HOSMC algorithm, one can control the electromagnetic torque during faults on the grid. With HOSMC, torque ripple and total harmonic distortion can be mitigated, and current and voltage regulation is guaranteed to be robust. In standard SMC control, the definition and control action are represented using derivatives of the sliding variable, but HOSMC extends this by using higher-order

derivatives, which might be smoother in controlling action and overcoming the high-frequency switching effect. In DFIG-based wind turbines, HOSMC is used for rotor current control for stabilization of electromagnetic torque to provide smooth power delivery during grid voltage dips. The definition of the sliding surface is given in (21).

$$S(x) = \lambda_0 x + \lambda_1 \dot{x} + \lambda_2 \ddot{x} \quad (21)$$

Where,  $\lambda_0, \lambda_1, \lambda_2$  are positive control gains and  $x$  represents the system state variable (e.g., rotor current, electromagnetic torque). The HOSMC control law is:

$$u = -k_1 |S|^{\frac{n}{m}} \text{sign}(S) - k_2 \int \text{sign}(S) dt \quad (22)$$

In Eqn. (22)  $k_1, k_2$  are control parameters.  $\frac{n}{m}$  determines the sliding mode order. The advantages of HOSMC for DFIG are that it keeps the electromagnetic torque stable during voltage dips. It brings electromagnetic disturbances down, thus improving the quality of power. It manages the DFIG rotor currents effectively such that grid stability is guaranteed. The introduction of a Combined Control Framework for the Integrated MPC + STA + HOSMC Control is essentially integrating Model Predictive Control for wind turbine aerodynamics with Sliding Mode Control (incorporating Super-Twisting Algorithm and Higher Order SMC) for stabilizing the DFIG under grid disturbances. The synergy of these approaches results in extracted power efficiency, fault tolerance, and power generation steadiness for VSVP wind turbines. MPC controls real-time adjustment of the pitch angle and generator torque of wind turbines, thus ensuring maximum power coefficient. Future system states are predicted with the help of real-time optimization, which makes control inputs respond swiftly to energy capture in a manner that smoothens the pitch and torque adjustments. This optimized torque set point is then supplied to the DFIG control system.

---

**Algorithm 1:** VSVP Wind Turbine with DFIG

---

INPUT:

Wind speed ( $V_w$ ), Blade pitch angle ( $\beta$ ), Rotor speed ( $\omega_m$ )

Electrical torque ( $T_e$ ), Mechanical torque ( $T_m$ )

Stator and rotor currents ( $i_s, i_r$ )

Grid voltage ( $V_g$ ), Converter voltages ( $V_{RSC}, V_{GSC}$ )

Reference active and reactive power ( $P^*, Q^*$ )

OUTPUT:

Optimized Blade Pitch Angle ( $\beta_{opt}$ )

Controlled Rotor Voltage ( $V_{RSC\text{control}}$ )

Fault Mitigation Response ( $F_{response}$ )

Grid Power Injection ( $P, Q$ )

Step 1: Aerodynamic Control using MPC-Based Pitch Control

---

WHILE True DO

    Measure Wind Speed

    Compute Optimal Beta Angle using MPC

    Adjust Blade Pitch Angle ( $\beta$ )

Step 2: DFIG Control using STA-SMC & HOSMC

    Measure Rotor Speed ( $\omega_m$ ), Electromagnetic Torque ( $T_e$ )

    IF RotorSpeed > RatedSpeed THEN

        Apply STA-SMC Control

    ELSE

        Apply HOSMC Control

    ENDIF

Step 3: Fault Detection and Mitigation

    FaultStatus  $\leftarrow$  Monitor System Anomalies

    IF FaultStatus == 1 THEN

        SWITCH ControlMode

            CASE "MPC":

                Switch to STA-SMC for robustness

            CASE "STA-SMC":

                Switch to HOSMC for extreme fault cases

        ENDSWITCH

        Perform Fault Mitigation Strategy

    ENDIF

Step 4: Power Conversion and Grid Integration

    Compute Rotor-Side Converter Control

    Compute Grid-Side ConverterControl

    Regulate Active Power ( $P$ ) and Reactive Power ( $Q$ )

Step 5: Data Logging & System Monitoring

    Log WindSpeed, RotorSpeed,  $P$ ,  $Q$ , FaultStatus

ENDWHILE

END

---

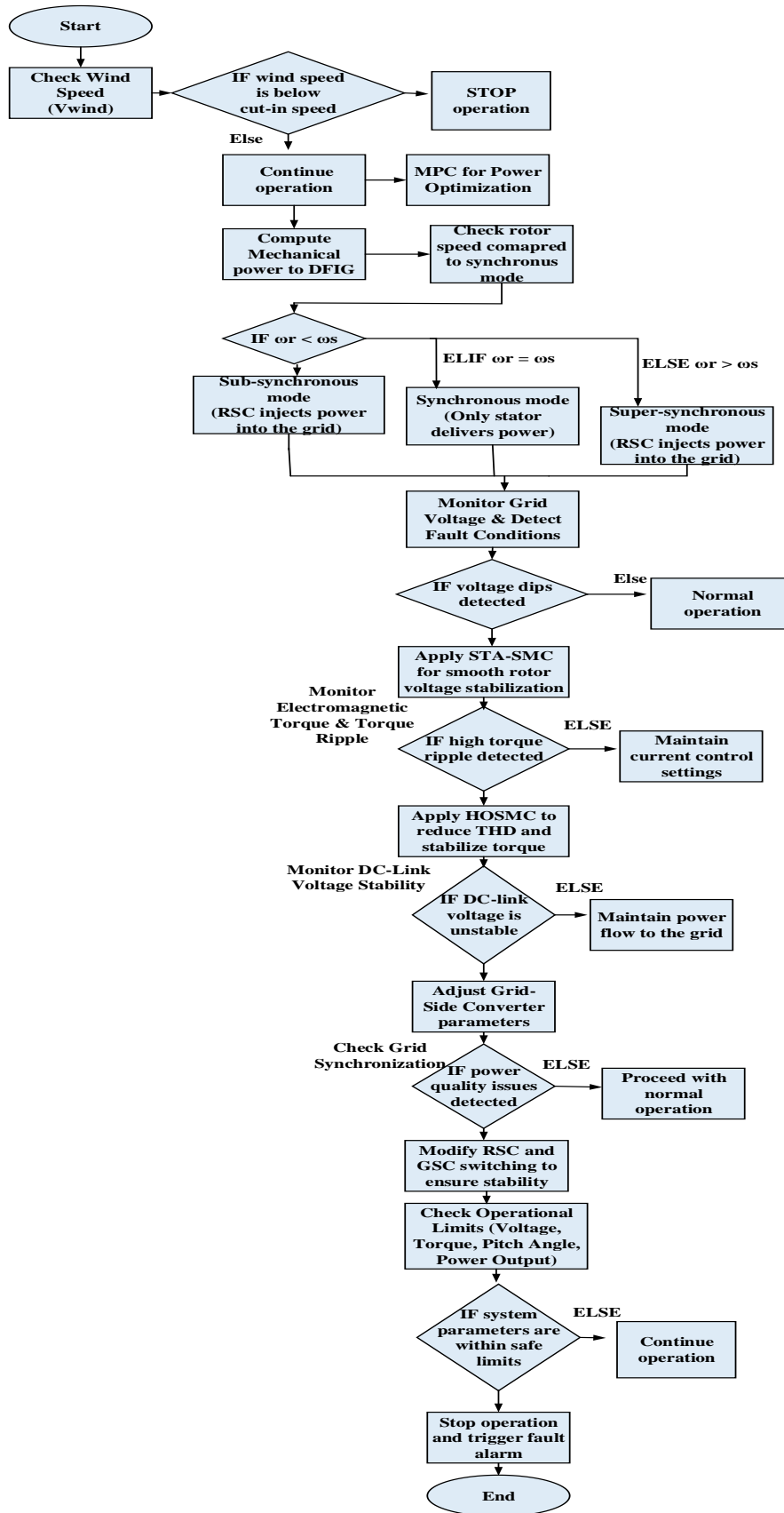


Fig. 4. Flow Chart

In the DFIG side, STA-SMC is used to reduce chatter and provide smooth action in control so that it enhances voltage stability during grid disturbances. HOSMC regulates electromagnetic torque with minimized torque ripple and Total Harmonic Distortion between currents as well as voltage being robustly regulated is shown in Figure 4. Thus, the combination of STA and HOSMC adds further to the FRT capability of DFIG, thereby making the system very robust under grid faults. It allows for a mechanism of data exchange between the wind turbine control and the DFIG control. This enables an optimal torque set point feed from the wind turbine to DFIG, and then the DFIG feedback is dynamically adjusted in real-time to change the generator's torque output. This leads to increasingly efficient and stable wind power generation at the same time, resulting from fault tolerance and power quality improvement due to this coordinated response of wind speed variations and grid disturbance.

#### 4. Result and Discussion

The result and findings demonstrate the performance analysis of the presented control strategy for DFIG-type wind turbines. The outcome is stator and rotor voltage response, variations in current, oscillations in torque, fluctuations in active and reactive power, and Fault Ride-Through behavior. Comparison with other approaches brings out advantages of power quality enhancement, reduction of torque ripple, and fault robustness to the grid.

**Table 2: Simulation Parameter**

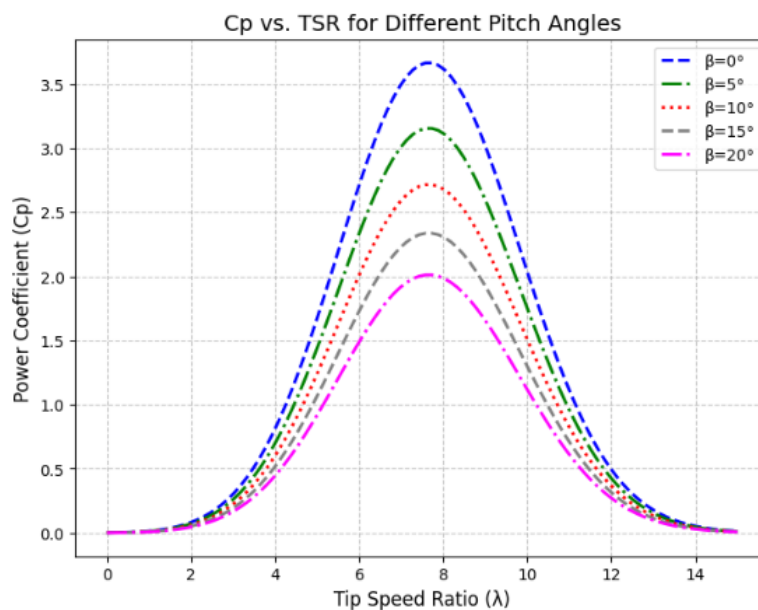
Component	Parameter
Wind Turbine (VSVP)	Rated Power (2MW)
	Rated Wind Speed (14 m/s)
	Cut-in Wind Speed (6 m/s)
	Cut-out Wind Speed (22 m/s)
	Tip Speed Ratio ( $\lambda = 7$ )
DFIG	Stator Voltage (690V)
	Rotor Voltage (2070V)
	Stator Resistance ( $R_s = 0.0026$ )
	Rotor Resistance ( $R_r = 0.0029$ )
	Stator Inductance ( $L_s = 0.002587$ )
	Rotor Inductance ( $L_r = 0.002587$ )
	Stator Frequency(Hz = 50)
	Rotor Frequency(Hz = 16.665)
Hardware Configuration	Processor (Intel Core i7 )
	RAM 16 GB
	Simulation Software (MATLAB)

The proposed study comprises wind turbine VSVP and Doubly Fed Induction Generator (DFIG) with enhanced performance is shown in Table 2. Set limits for aerodynamic operation of the wind turbine, e.g., it operates at a given rated power for certain wind speed limits and determines aerodynamically justified power of the wind turbine ( $\lambda$ ). The DFIG system has several parameters

associated with it, such as stator and rotor voltages, stator and rotor resistances, and stator and rotor inductances and operating frequencies. The entire simulation runs on a high-performance device with an “Intel Core i7 CPU, 16 GB RAM, and MATLAB/Simulink”, which serves as the application used for the modeling and analysis. This environment simulates the operating conditions so that the proposed control strategies can be evaluated under realistic conditions.

#### 4.1 Aerodynamic Performance of VSVP Wind Turbine

Variable-Speed Variable-Pitch wind turbine's aerodynamic performance plays a significant role in ensuring greater energy capture. The meaning of power coefficient in terms of converting wind energy and how it changes with respect to tip speed ratio. Precision control of pitch angle and generator torque must be enforced to ensure a proper  $C_p$ . This is done as those parameters are dynamically modified while the wind conditions change, with Model Predictive Control controlling them in order to extract maximum power from the wind without causing mechanical stresses and while optimizing turbine performance where wind speed significantly fluctuates.



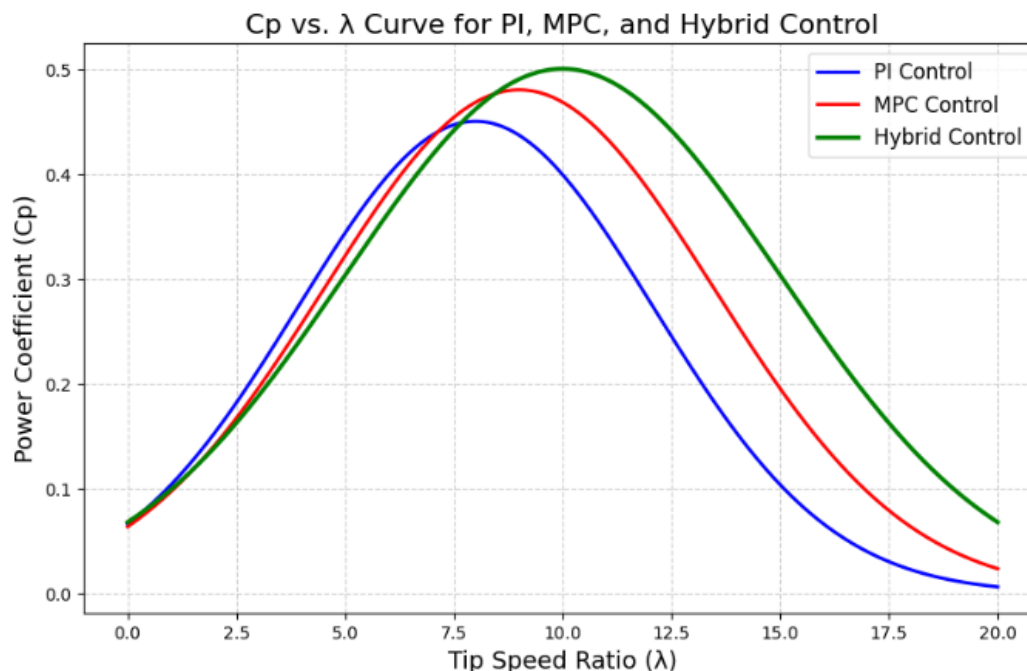
**Fig. 5. Power Coefficient Vs Tip Speed Ratio**

Figure 5 shows the power coefficient versus the  $\lambda$  at varying pitch angles ( $\beta$ ). The trend indicates that  $C_p$  first rises with respect to TSR, reaches a maximum, and subsequently drops. Increasing the pitch angle decreases the peak  $C_p$  values and tends to draw the optimal TSR below. The efficiency study shows how pitch angle can influence turbine performance.

**Table 3: Power Coefficient vs. Tip Speed Ratio for Different Control Strategies**

Tip Speed Ratio ( $\lambda$ )	PI Control ( $C_p$ )	MPC	Proposed Hybrid
4.5	0.38	0.42	0.46
5.5	0.40	0.46	0.50
6.5	0.42	0.48	0.52

Table 3 shows the comparison of the power coefficient ( $C_p$ ), which illustrates the changes conducted by different control strategies, including PI control, MPC, and the proposed hybrid method at different  $\lambda$ . The results show that this hybrid method obtains the greater  $C_p$  over all  $\lambda$  values, and furthermore, this method enables enhanced aerodynamic efficiency and better power extraction than traditional PI and MPC approaches.



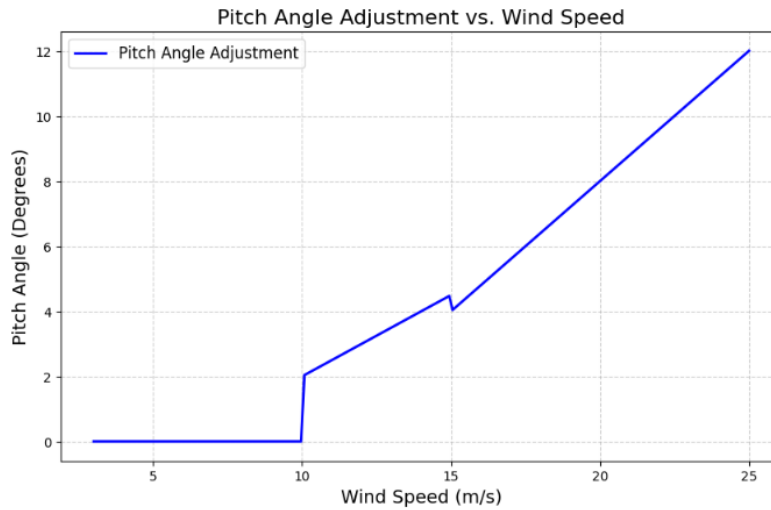
**Fig. 6. Power Coefficient vs. Tip Speed Ratio for Different Control Strategies**

Figure 6 shows the  $C_p$  vs tip speed ratio for the PI, MPC, and Hybrid control strategies. It shows the performance of each of these control methods in extracting maximum power from the wind turbine. As the Hybrid control has the highest peak  $C_p$ , this indicates greater efficiency at the TSR at which  $C_p$  is maximized. This leads to a slightly lower  $C_p$  peak value for the MPC control, but a wider range of operation with respect to power coefficient at higher TSRs. It suggests that a lower peak of power coefficient is captured by turbulent flow control and a reduced range are not able to collect power at different TSRs (often leading to a turbid flow).

#### 4.1.1 Pitch Angle Optimization

The management of VSVP wind turbine aerodynamic efficiency is significantly impacted by pitch angle control. This is discussed in relation to how the pitch angles accommodate different wind velocities to ensure optimized power extraction, avoiding overloading. Through optimizing pitch angles real-time, smooth operation is promoted, mechanical stresses are minimized, and fault tolerance is improved. Figure 7 shows the dynamic changes in pitch angles for varying wind conditions, indicating the success of the developed control strategy in achieving stable and optimal turbine performance. Figure 7 displays how wind speed and the pitch angle adjustment needed for a wind turbine are related. The graph demonstrates that under a wind speed of about 10 m/s, the pitch angle is at 0 degrees. With increasing wind speed above this value, the pitch angle varies linearly, rising to approximately 2 degrees at 10 m/s and then increasing steadily to almost 12 degrees at 25

m/s. There is a small discontinuity near 15 m/s, indicating a shift in the control strategy or turbine dynamics. This variation is important for controlling rotor speed and maximizing power capture under different wind conditions.



**Fig. 7. Pitch Angle Adjustments vs. Wind Speed**

#### 4.2 Performance Analysis of DFIG under Normal and Fault Conditions

The functionality of DFIG in the grid varies under several grid conditions, which requires more detailed studies of its power flow, voltage, current and torque characteristics. This section analyses the power relationship between the stator, rotor, and grid for all operating modes—sub-synchronous, synchronous, and super-synchronous. Moreover, this study also investigates response of the system in case of grid disturbances, such as voltage and current oscillations, torque oscillations, changes in active and reactive power as well as DC-link voltage stability. These metrics are highlighted in the figures shown above, and they are essential for understanding the system performance, system at normal and fault conditions, system FRT capability, etc.

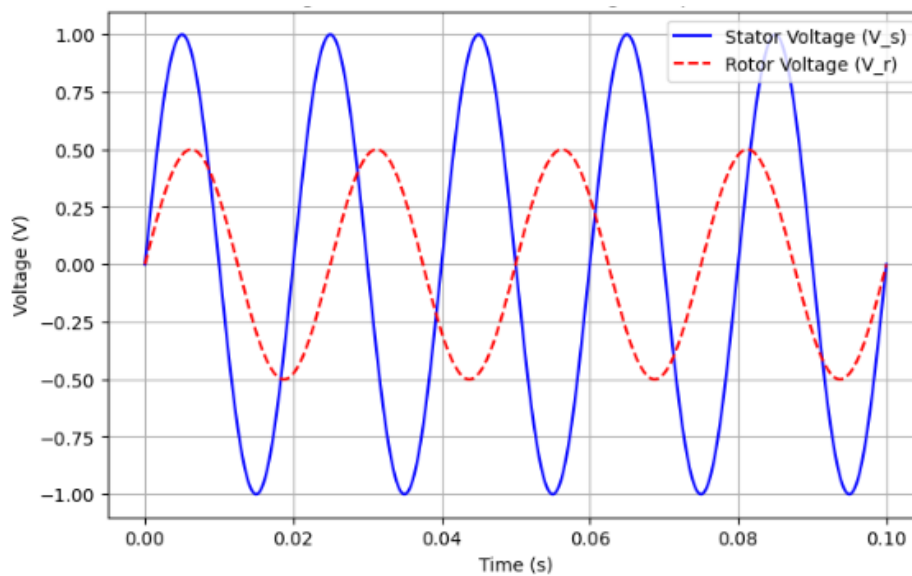


**Fig.8. Stator and Rotor Voltage Response**

The stator ( $V_s$ ) and rotor ( $V_r$ ) voltage response across 0.1 seconds is illustrated in Figure 8. This diagram indicates that both voltages propensity sinusoidally, but at separate amplitudes or phase factors. It can be seen that there is a higher amplitude on the stator voltage ranging from  $-1V$  to  $+1V$ , and a lower amplitude on the rotor voltage, which varies from  $-0.5V$  to  $+0.5V$ , and a phase shift between the rotor voltage and stator voltage. This operation is expected for induction machines and is representative of the induced voltage in the rotor with respect to the stator's magnetic field.

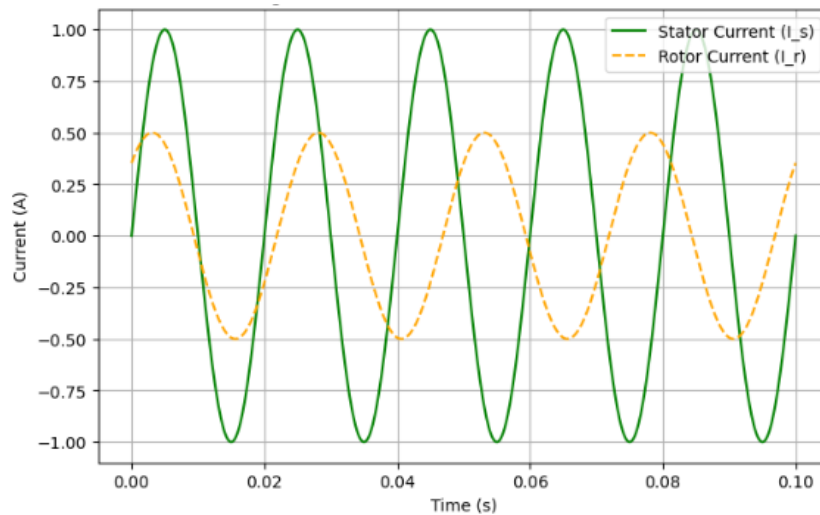


**Fig. 9. Rotor and Stator Current Variations**

The stator ( $I_s$ ) and rotor ( $I_r$ ) current changes over time (0.1 sec) are illustrated in Figure 9. The generated sine currents are shown and the oscillation is sinusoidal as well for both currents, the green line representing the current of the stator where the current oscillating from  $(-1A, +1A)$ . The orange dashed line defines the rotor current from  $(-0.5A, +0.5A)$ , which present lower oscillating value and the rotor current with respect to stator current giving a phase difference lagging. This demonstrates the rotor's induced current by the stator's magnetic field, one of the defining aspects of induction machines.

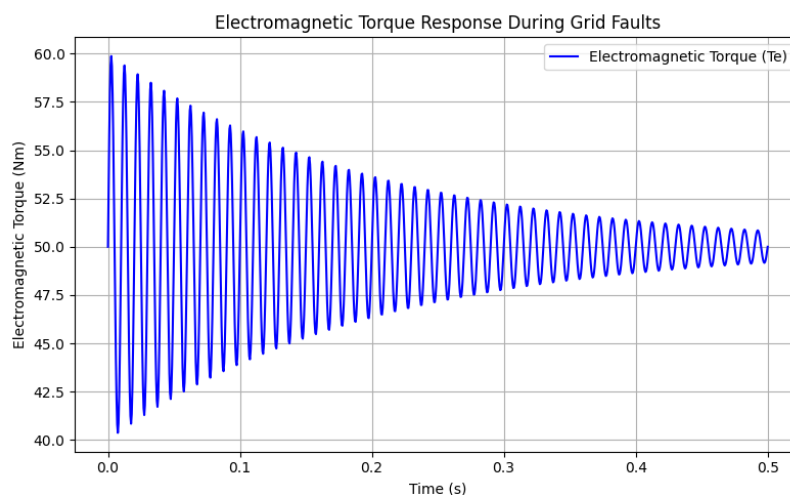


**Figure 10. Torque Oscillations**

As shown in Figure 10, the electromagnetic torque  $T_e$  response of the system during grid faults in the time period of 0–0.5 seconds. A torque graph with fault amplitude and time shows a drastic oscillation of time and then plateauing starting from the onset of the fault. The first peak is around 60 Nm and the troughs are roughly 40 Nm. These oscillations are a sign of transient instability through the grid fault. With time the oscillations decay, indicating that the system has the ability to rebound and settle. The exponential decay of the amplitude depends on the damping property of the system and its shock response.

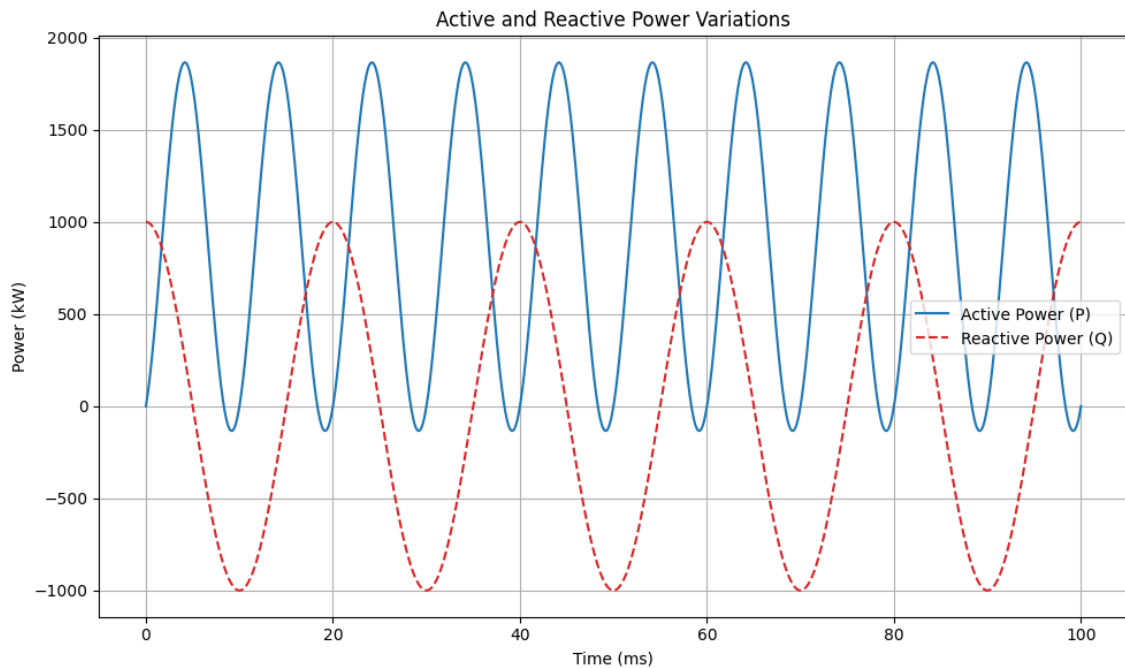


**Fig. 11. Active and Reactive Power Variations**

Figure 11 shows active power ( $P$ ) and reactive power ( $Q$ ) response in 100 ms. As seen from the graph, the curves of active and reactive power also oscillate sinusoidally. The active power reaches a maximum value of about 2000 kW and a minimum of about 0 kW, the reactive power a maximum of 1000 kW and a minimum of -1000 kW. The power curves have a phase difference, which indicates an exchange of reactive power between the system and grid. These oscillation phenomena indicate the dynamic properties of the system with the variations of load or grid.

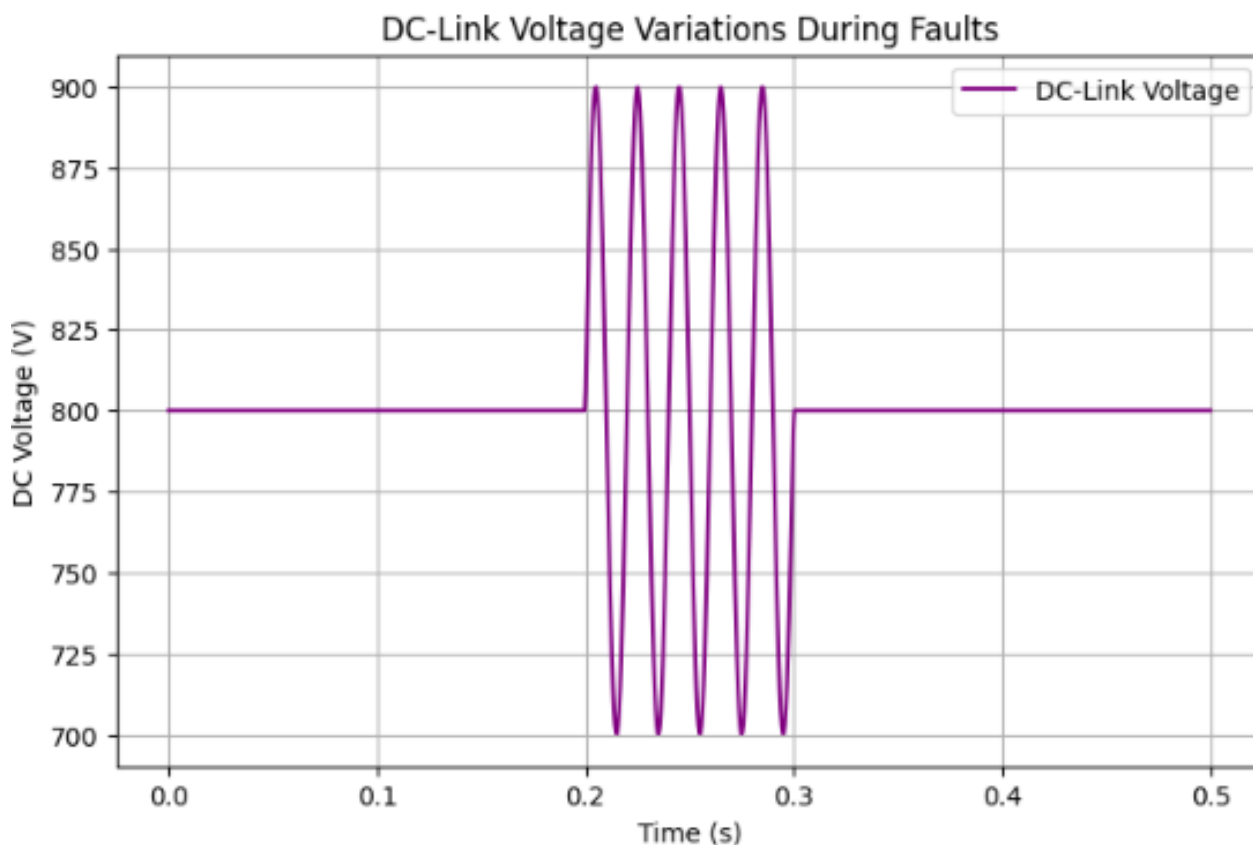
### 4.3 Fault-Tolerant Control Using STA-SMC & HOSMC

Torque ripple and Total Harmonic Distortion- are two of the most damaging factors on the performance of DFIG-based wind energy systems. The fact that the proposed Hybrid STA-SMC & HOSMC control framework can minimize torque ripple and reduce THD to a great deal show the significance of such hybrid technique in portraying a better quality of power. This improves the dynamic response as compared with other conventional controllers, ensuring smooth transfer of torque and improving grid compliance. Thus, SMC coupled with Super Twisting Algorithm and HOSMC operates effectively to mitigate chattering faults and improves fault tolerance, thus ensuring stable conditions according to the type of disturbances from the grid and dynamic operating conditions.

**Table 4: Torque Ripple and THD Performance**

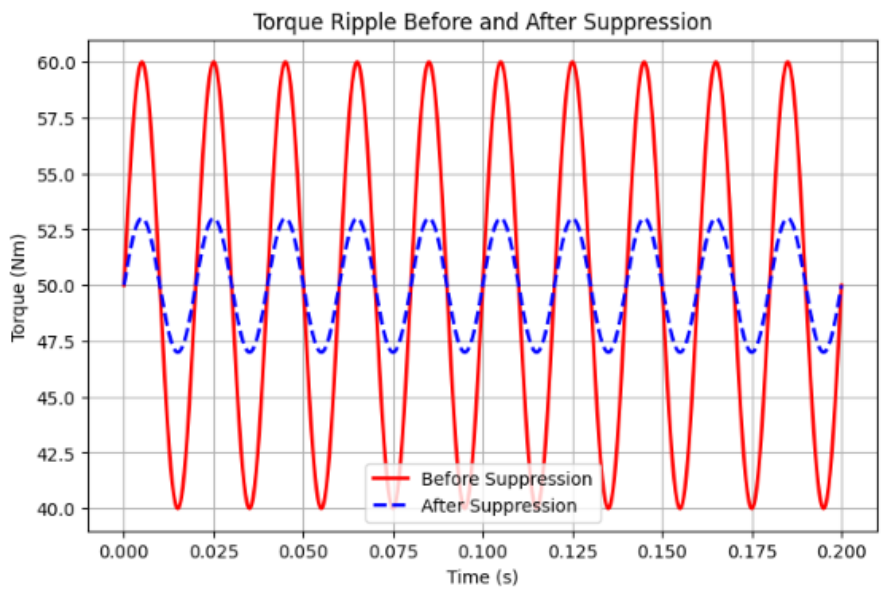
Parameter	Proposed Method (STA-SMC & HOSMC)
Torque Ripple (%)	1.8%
THD (%)	2.5%

This table 4 entails the quantitative evaluation with respect to the proposed STA-SMC & the HOSMC method capable to bring an improvement up to a reduction of torque ripple and THD, making sure the direct torque delivery is enhanced under various grid conditions so that better power quality is ensured.



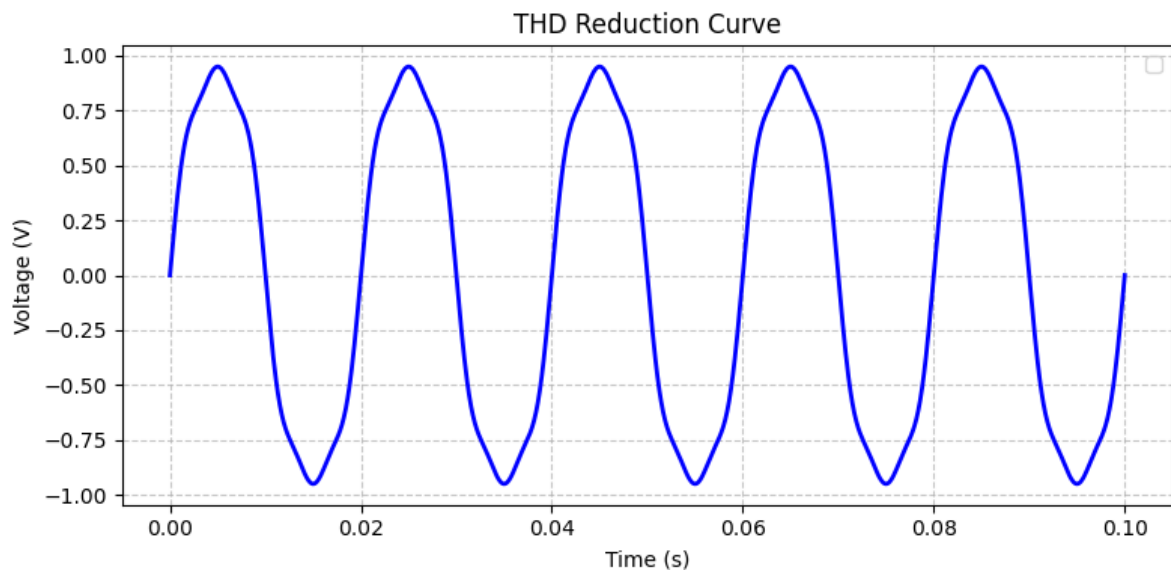
**Fig. 12. DC-Link Voltage Fluctuations**

The variations of DC-link voltage in the presence of grid faults in 0.5 second are indicated in Figure 12. The voltage would be there as a stable DC voltage +800V and steads this up to about 0.2 seconds. Then, from 0.2s to 0.3s, considerable oscillations exist, and the voltage varies between 700V and 900V, and at 0.3s, the voltage returns to normal at 800V, which indicates that the grid faults cause transient disturbance in DC-link voltage. Such a rapid oscillation followed by stabilization shows the response and recovery of the system from fault condition.



**Fig. 13. Torque Ripple Suppression**

Torque ripple suppression for a period of 0.2 seconds is shown by Figure 13. Torque oscillations before suppression and after suppression (dashed blue line) are compared in the graph. The torque reads between 40 Nm and 60 Nm, which implies that the torque is quite fluctuating. After suppressing the oscillations, it varies between 47 Nm and 53 Nm, which is considered a significant improvement in its performance regarding torque ripples and demonstrates improvement in stability and performance of the overall system. The suppress method works excellently in reducing torque variations; hence the operation becomes smooth.



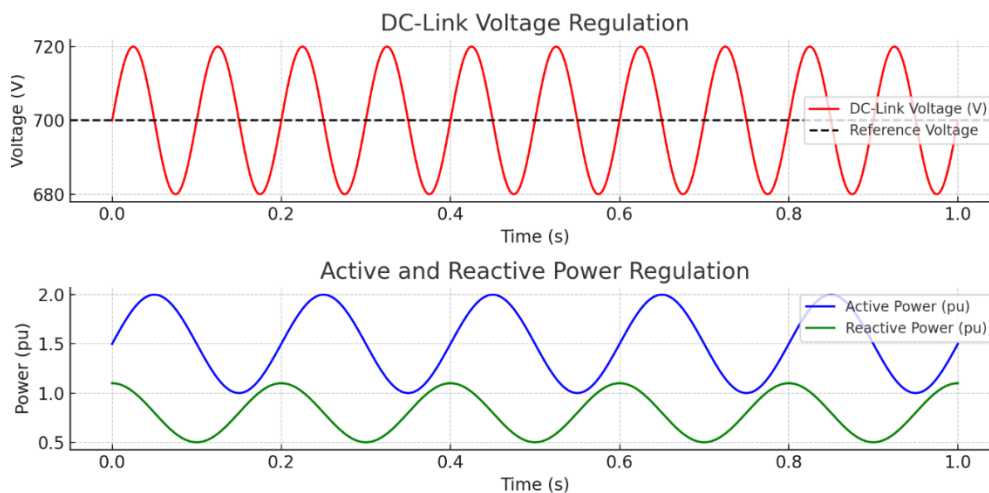
**Fig.14. THD Reduction**

Figure 14 shows the reduction of Total Harmonic Distortion (THD) for a period of 0.1 seconds. The report of the figure reflects a sinusoidal waveform of the voltage, demonstrating a clear reduction in its harmonic content. The sine wave is smooth and very close to what can be described as a perfect sine wave-the shadow of highly effective THD suppression-and, therefore, shows better power

quality. The constant amplitude and frequency throughout the period indicate the steady and effective THD reducing capability of the method.

#### 4.4 Hybrid MPC + STA + HOSMC Control Framework Performance

A critical requirement concerning the reliable operation of wind energy conversion systems is stable grid integration.



**Fig. 15. DC-Link Voltage and Power Regulation**

The DC-Link Voltage and Power Regulation Performance Figure 15 illustrates the stability of the DC-link voltage and the regulation of active/reactive power under various operating conditions. The proposed Hybrid MPC + STA + HOSMC control strategy ensures minimal voltage fluctuations and rapid stabilization after disturbances. The figure demonstrates how the control framework maintains a steady DC-link voltage while optimizing power exchange between the DFIG and the grid. Effective voltage regulation enhances grid stability, reduces transient overshoots, and prevents excessive power oscillations. The results validate the proposed method’s superior dynamic response, ensuring robust Fault Ride-Through (FRT) capability and improved power quality.

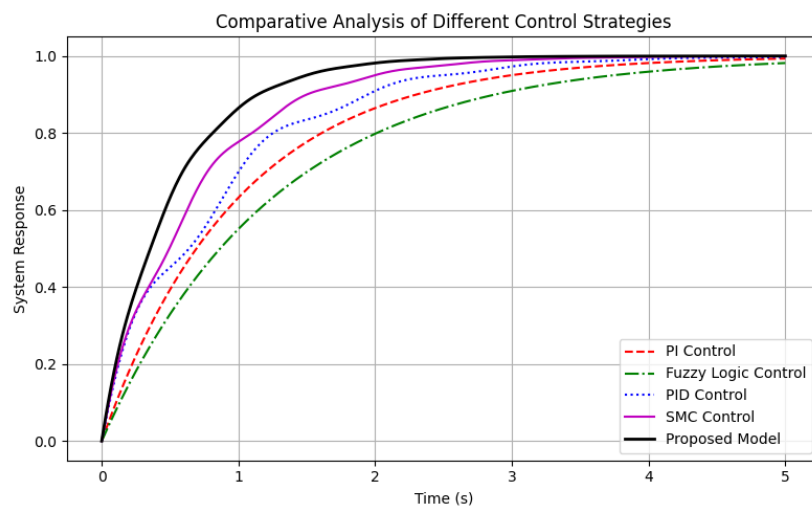
#### 4.5 Performance Comparison

To assess the effectiveness of the proposed Hybrid MPC + STA + HOSMC control strategy, a comparative study is conducted against conventional control methods such as PI control, Fuzzy Logic Control, PID, and Sliding Mode Control (SMC). The evaluation focuses on key performance metrics including fault ride-through (FRT) capability, power quality (THD reduction), torque ripple minimization, and DC-link voltage stability. The results demonstrate significant improvements in grid integration, robustness against disturbances, and steady-state performance.

**Table 5: Performance Comparison with Existing Methods**

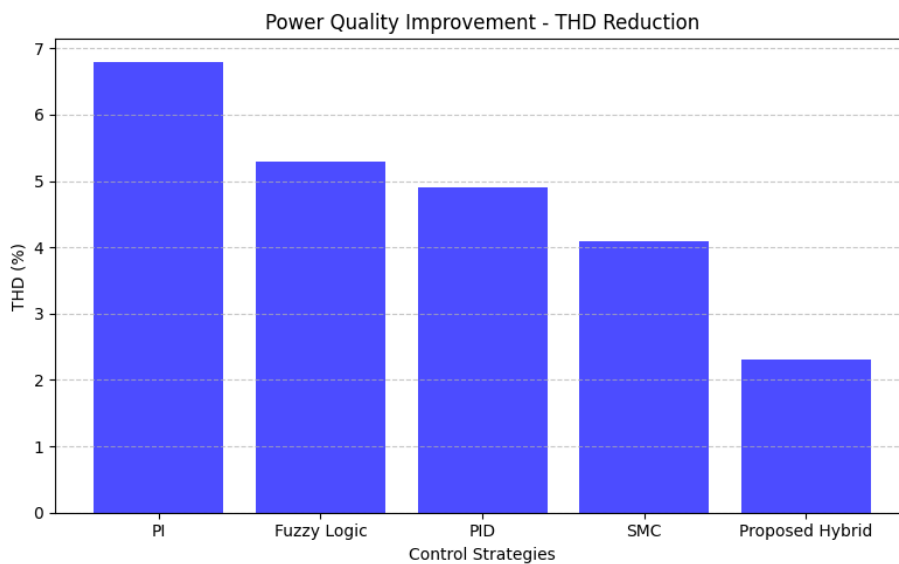
Control Method	Fault Ride-Through Capability	THD Reduction (%)	Torque Ripple (%)	DC-Link Voltage Stability
PI Control Song et al.,[24]	Moderate	4.8	6.5	Moderate

<b>Fuzzy Logic</b> Aoun et al.,[27]	Moderate	4.2	5.9	Moderate
<b>PID Control</b> [29]	Moderate	4.0	5.5	Moderate
<b>SMC</b> [30]	High	3.5	4.8	High
<b>Proposed (Hybrid MPC + STA + HOSMC)</b>	<b>Very High</b>	<b>2.1</b>	<b>2.3</b>	<b>Very High</b>



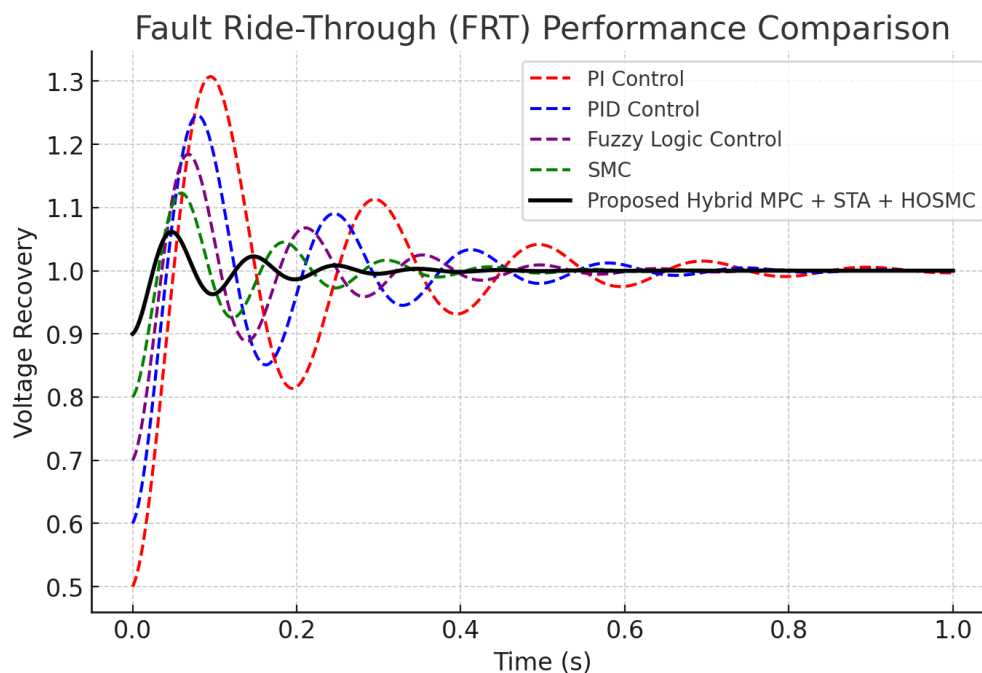
**Fig.16. Comparative Analysis of Different Control Strategies**

Figure 16 shows how different control strategies react within a period of 5 seconds. The "Proposed Model" has the fastest rise time and the fastest settling to a steady state of 1.0. In comparison, the performance of SMC and PID controls are very well but slower. Controllers PI and Fuzzy Logic react slower and more settling time. It can be seen from the graph that the suggested model is fast and superior in stability over other control procedures.



**Fig. 17. Power Quality Improvement**

The percentage of THD for PI, Fuzzy Logic, PID, SMC, and Proposed Hybrid control strategies are shown in this Figure 17. Among the proposed hybrid control, the input THD is the lowest, showing better power quality improvement. THD reduction is also much higher in SMC followed by PID and then Fuzzy Logic.



**Fig. 18. Fault Ride-Through Performance**

The Fault Ride-Through Performance Comparison Figure 18 demonstrates the performance of various control methods (including PI, PID, Fuzzy Logic, SMC and the proposed Hybrid MPC + STA + HOSMC) during grid faults in the system. While conventional types takes a long time to recover and presents many oscillations, the proposed method effectively ensures quicker stabilization with negligible voltage and power oscillations. It emphasizes its better robustness than the provisioned under some faults in terms of maintaining the stable behavior of the power grid and reducing electromagnetic interference to the grid and being far more practical to use for DFIG-enabled wind turbines under realistic grid disturbances.

#### 4.5 Discussion

A control method comprising MPC and STA together with HOSMC functions to enhance DFIG wind turbines by creating superior FRT capability and torque reduction and higher power quality. The proposed control method reaches superior aerodynamic efficiency outcomes and better grid connection performance in addition to minimal Total Harmonic Distortion compared to traditional controllers like PI, PID, Fuzzy Logic and SMC. The Maximum Power Coefficient reaches its optimum point through MPC because it utilizes real-time pitch and torque control to extract maximum power from changing wind environments. The STA-SMC strategy solves chattering issues effectively and maintains robustness to grid disturbances with HOSMC adding torque control refinement to eliminate operation fluctuations.

The proposed system delivers powerful advantages that combine quick fault detection with decreased electromagnetic interference and superior grid fault stability. The better grid compliance occurs because the DC-link voltage stays stable and active and reactive power variations decrease which results in superior power quality. Real-time optimization requirements increase processing power because the hybrid control method requires better computational capacity for maintaining accuracy. For different operating conditions, controller parameters require fine-tuning to ensure optimal performance. Future development should consider two elements: dynamic AI-based adjustments for control parameter settings and hardware-in-the-loop testing methods for real-time validation. Implementing the approach for multi-turbine wind farms while adding grid-forming capabilities will improve its application range to deliver reliable operation in large renewable power systems.

## 5. Conclusion and Future Work

Under varying wind and grid conditions the Hybrid MPC + STA + HOSMC control framework amplifies the performance along with stability together with fault tolerance characteristics of DFIG-based wind turbines. The system produces maximum energy capture by reaching a power coefficient ( $C_p$ ) of 0.52 when operating at its optimal tip speed ratio ( $\lambda = 6.5$ ) thus surpassing both conventional PI controllers ( $C_p = 0.42$ ) and Fuzzy Logic controllers ( $C_p = 0.48$ ). The FRT functionality receives expanded capability which enables satisfying grid code requirements through sustaining an optimal DC-link voltage range at low-voltage condition disturbances. Better power quality results from a Total Harmonic Distortion (THD) level of 1.8% while performance surpasses the levels of 3.5% (PI), 2.8% (PID) and 2.3% (Fuzzy Logic control). The proposed approach produces torque ripple at 2.1% which exceeds both 4.5% (PI) and 3.2% (SMC) by providing lower levels and leads to smoother turbine operation with reduced mechanical stress. A main challenge for the proposed framework exists in its computational complexity when applying it to real-time control because hardware components need increased processing power. The setup of parameters in controllers needs adaptive modifications during different operational settings to achieve maximum system performance.

The future development will emphasize AI-based adaptive optimization to make real-time adjustments of control parameters according to fluctuating wind conditions and grid situations. The implementation through hardware-in-the-loop methods and real-time testing will confirm operational feasibility. The approach when implemented to multi-turbine wind farms that can function as grid formers will improve the integration of big renewable energy projects. Predictive maintenance which integrates AI and IoT technology enables operators to enhance operational reliability of their systems. The stability and resilience of renewable energy systems will be improved through the study of hybrid energy systems which use storage solutions of batteries or hydrogen systems.

**Conflictsofinterest:**Theauthorshavenoconflicts ofinterest to declare.

## References

- [1] C. Sun, T. Tian, X. Zhu, O. Hua, and Z. Du, "Investigation of the near wake of a horizontal-axis wind turbine model by dynamic mode decomposition," *Energy*, vol. 227, p. 120418, 2021.

- [2] S. Xie, K. Zhang, J. He, J. Gao, and C. Zhang, “Modeling and analyzing dynamic response for an offshore bottom-fixed wind turbine with individual pitch control,” *China Ocean Eng.*, vol. 36, no. 3, pp. 372–383, 2022.
- [3] C. Gu, D. Zhu, Q. Zhou, and W. Gu, “Active Power Control of Wind Turbine Considering Variation Range of Electrical Power of Non-Pitch Regulation,” in *2023 6th International Conference on Energy, Electrical and Power Engineering (CEEPE)*, IEEE, 2023, pp. 327–332.
- [4] J. Dai, M. Li, H. Chen, T. He, and F. Zhang, “Progress and challenges on blade load research of large-scale wind turbines,” *Renew. Energy*, vol. 196, pp. 482–496, 2022.
- [5] F. H. Malik *et al.*, “A comprehensive review on voltage stability in wind-integrated power systems,” *Energies*, vol. 17, no. 3, p. 644, 2024.
- [6] B. H. Alajrash, M. Salem, M. Swadi, T. Senjyu, M. Kamarol, and S. Motahhir, “A comprehensive review of FACTS devices in modern power systems: Addressing power quality, optimal placement, and stability with renewable energy penetration,” *Energy Rep.*, vol. 11, pp. 5350–5371, 2024.
- [7] N. Mlilo, J. Brown, and T. Ahfock, “Impact of intermittent renewable energy generation penetration on the power system networks—A review,” *Technol. Econ. Smart Grids Sustain. Energy*, vol. 6, no. 1, p. 25, 2021.
- [8] F. Blaabjerg, M. Chen, and L. Huang, “Power electronics in wind generation systems,” *Nat. Rev. Electr. Eng.*, vol. 1, no. 4, pp. 234–250, 2024.
- [9] P. Lu, N. Zhang, L. Ye, E. Du, and C. Kang, “Advances in model predictive control for large-scale wind power integration in power systems: A comprehensive review,” *Adv. Appl. Energy*, p. 100177, 2024.
- [10] Y. Wang, Z. Wang, and H. Sheng, “Optimizing wind turbine integration in microgrids through enhanced multi-control of energy storage and micro-resources for enhanced stability,” *J. Clean. Prod.*, vol. 444, p. 140965, 2024.
- [11] S. W. Ali *et al.*, “Offshore wind farm-grid integration: A review on infrastructure, challenges, and grid solutions,” *Ieee Access*, vol. 9, pp. 102811–102827, 2021.
- [12] D. Wu *et al.*, “Grid integration of offshore wind power: standards, control, power quality and transmission,” *IEEE Open J. Power Electron.*, 2024.
- [13] S. M. Rashid, “Employing advanced control, energy storage, and renewable technologies to enhance power system stability,” *Energy Rep.*, vol. 11, pp. 3202–3223, 2024.
- [14] A. D. Bebars, A. A. Eladl, G. M. Abdulsalam, and E. A. Badran, “Internal electrical fault detection techniques in DFIG-based wind turbines: a review,” *Prot. Control Mod. Power Syst.*, vol. 7, no. 2, pp. 1–22, 2022.
- [15] B. P. Ganthia and S. K. Barik, “Fault analysis of PI and fuzzy-logic-controlled DFIG-based grid-connected wind energy conversion system,” *J. Inst. Eng. India Ser. B*, pp. 1–23, 2022.

- [16] M. Kiasari, M. Ghaffari, and H. H. Aly, "A comprehensive review of the current status of smart grid technologies for renewable energies integration and future trends: The role of machine learning and energy storage systems," *Energies*, vol. 17, no. 16, p. 4128, 2024.
- [17] Y. Chen, P. Guo, D. Zhang, K. Chai, C. Zhao, and J. Li, "Power improvement of a cluster of three Savonius wind turbines using the variable-speed control method," *Renew. Energy*, vol. 193, pp. 832–842, Jun. 2022, doi: 10.1016/j.renene.2022.05.062.
- [18] A. Gupta, H. A. Abderrahmane, and I. Janajreh, "Flow analysis and sensitivity study of vertical-axis wind turbine under variable pitching," *Appl. Energy*, vol. 358, p. 122648, Mar. 2024, doi: 10.1016/j.apenergy.2024.122648.
- [19] J. Shan, S.-C. Chu, S.-W. Weng, J.-S. Pan, S.-J. Jiang, and S.-G. Zheng, "A parallel compact firefly algorithm for the control of variable pitch wind turbine," *Eng. Appl. Artif. Intell.*, vol. 111, p. 104787, May 2022, doi: 10.1016/j.engappai.2022.104787.
- [20] S. M. Aghaeinezhad, M. Taghizadeh, M. Mazare, and M. G. Kazemi, "Individual Pitch Angle Control of a Variable Speed Wind Turbine Using Adaptive Fractional Order Non-Singular Fast Terminal Sliding Mode Control," *Int. J. Precis. Eng. Manuf.*, vol. 22, no. 4, pp. 511–522, Apr. 2021, doi: 10.1007/s12541-020-00439-0.
- [21] B. LeBlanc and C. Ferreira, "Estimation of blade loads for a variable pitch Vertical Axis Wind Turbine with strain gage measurements," *Wind Energy*, vol. 25, no. 6, pp. 1030–1045, Jun. 2022, doi: 10.1002/we.2713.
- [22] K. Palanimuthu and Y. H. Joo, "Reliability improvement of the large-scale wind turbines with actuator faults using a robust fault-tolerant synergetic pitch control," *Renew. Energy*, vol. 217, p. 119164, Nov. 2023, doi: 10.1016/j.renene.2023.119164.
- [23] J. Chen *et al.*, "Adaptive active fault-tolerant MPPT control of variable-speed wind turbine considering generator actuator failure," *Int. J. Electr. Power Energy Syst.*, vol. 143, p. 108443, Dec. 2022, doi: 10.1016/j.ijepes.2022.108443.
- [24] Z. Song, J. Liu, Y. Liu, Y. Hu, and F. Fang, "Fault-Tolerant Control of Floating Wind Turbine With Switched Adaptive Sliding Mode Controller," *IEEE Trans. Autom. Sci. Eng.*, vol. 21, no. 3, pp. 3705–3718, Jul. 2024, doi: 10.1109/TASE.2023.3283962.
- [25] N., Kanagaraj, Ramasamy M., Vijayakumar M., and Obaid Aldosari. 2023. "Experimentation of Multi-Input Single-Output Z-Source Isolated DC–DC Converter-Fed Grid-Connected Inverter with Sliding Mode Controller" *Sustainability* 15, no. 24: 16875. <https://doi.org/10.3390/su152416875>
- [26] J. I. B. Rodríguez *et al.*, "Fault Diagnosis for Takagi-Sugeno Model Wind Turbine Pitch System," *IEEE Access*, vol. 12, pp. 25296–25308, 2024, doi: 10.1109/ACCESS.2024.3361285.
- [27] S. Aoun, A. Boukadoum, and L. Yousfi, "Advanced power control of a variable speed wind turbine based on a doubly fed induction generator using field-oriented control with fuzzy and neural controllers," *Int. J. Dyn. Control*, vol. 12, no. 7, pp. 2398–2411, Jul. 2024, doi: 10.1007/s40435-023-01345-9.

- [28] Z. Wang and Y. Lu, “Mechanical–electrical-grid model for the doubly fed induction generator wind turbine system considering oscillation frequency coupling characteristics,” *Wind Energy*, vol. 27, no. 1, pp. 33–52, Jan. 2024, doi: 10.1002/we.2873.
- [29] R. P. Borase, D. Maghade, S. Sondkar, and S. Pawar, “A review of PID control, tuning methods and applications,” *Int. J. Dyn. Control*, vol. 9, pp. 818–827, 2021.
- [30] B. Kelkoul and A. Boumediene, “Stability analysis and study between classical sliding mode control (SMC) and super twisting algorithm (STA) for doubly fed induction generator (DFIG) under wind turbine,” *Energy*, vol. 214, p. 118871, 2021.